

Etherification of aldehydes, alcohols and their mixtures on Pd/SiO₂ catalysts

Trung T. Pham, Steven. P. Crossley, Tawan Sooknoi, Lance L. Lobban,
Daniel E. Resasco, Richard G. Mallinson*

School of Chemical, Biological and Materials Engineering, University of Oklahoma, 100 Boyd St, T-335, Norman, OK 7301, United States

ARTICLE INFO

Article history:

Received 10 December 2009
Received in revised form 2 March 2010
Accepted 7 March 2010
Available online 12 March 2010

Keywords:

Etherification
Hydrogenation
Decarbonylation
Aldehyde
Alcohol

ABSTRACT

Dialkyl ethers have been selectively produced from etherification of aldehydes and alcohols on supported Pd catalysts. A yield of 79% ether with a selectivity of 90% was observed when feeding 2-methylpentanal with 2-methylpentanol at a molar ratio 1:1 at 125 °C. Cross etherification of n-butanol with 2-methylpentanal shows a much higher rate than that observed when the alcohol or aldehyde is fed alone. This enhanced activity is in line with the catalyst requirement for large ensembles that allow surface alkoxide species next to η^2 adsorbed aldehydes. Etherification when only aldehyde or alcohol is fed arises predominantly due to aldehyde–alcohol inter-conversion to produce the necessary co-reactant. The ether yield at the same reaction conditions decreases with metal loading in the order 16 > 10 > 3 wt.% Pd. Increasing reduction temperature also increases ether yield. It is apparent that etherification is highly sensitive to metal particle morphology, consistent with needing ensembles that accommodate the two adjacent adsorption sites.

© 2010 Elsevier B.V. All rights reserved.

1. Introduction

Biofuel production has attracted substantial attention in recent years [1–4]. There is strong motivation to produce fuels from oxygenated molecules generated from biomass conversion. Much research has been focused toward production of fungible molecules that may be readily incorporated into the existing transportation fuel infrastructure. Ethers are one of the potential fuel components made from oxygenates that might be used either in gasoline or diesel blends. Ethers were first commercially introduced in Italy in 1973 as a blending component in gasoline [5]. More recently, Olah [6] patented the use of C₂–C₂₄ alkyl ethers as blending components for diesel fuels, demonstrating cetane number improvement from 2 to 20 points. Use of short alkyl ethers such as methyl-t-butylether (MTBE), methyl-t-amylether (TAME) and ethyl-t-butylether (ETBE) as fuel additives have had negative environmental impact due to their high solubility in water that enhances their dispersion in the environment. These problems are much less severe with larger alkyl ethers, which exhibit much lower solubility. However, despite their excellent combustion and physical properties [7,8], overcoming perceived environmental issues will be required before ethers can be added to the fuel pool.

Alcohol etherification on acid catalysts is a well-established reaction [5,9–12]. Much less attention has been received to the study of ether formation on metal catalysts [13–18]. While studies focusing on etherification of alcohol and aldehyde have identified the need for ensembles of sites to accomplish the condensation [14–16], the influence of metal surface structure on ether selectivity has not been demonstrated in a systematic way.

In recent work [19], we have shown that 2-methylpentanal may be selectively produced from hydrogenation of 2-methyl-2-pentenal, itself produced from aldol condensation of glycerol or from propanal. These compounds are representative of types of bio-derived aldehydes and analogous alcohols from processes such as biomass pyrolysis. The present contribution investigates the etherification of 2-methylpentanal to form di-2-methylpentylether (DMPE) on Pd catalysts of varying particle size and morphology to help understanding the pathways of etherification of smaller bio-derived oxygenates by metal catalysts.

2. Experimental

2.1. Catalyst synthesis

Different loadings (3, 10 and 16 wt.%) of Pd catalysts were prepared by incipient wetness impregnation of the metal precursor on precipitated silica (HiSil 210 obtained from Pittsburgh Plate Glass Co.) having a BET surface area of 124 m²/g. The metal loading on each catalyst was calculated based on the amount of metal pre-

* Corresponding author. Tel.: +1 4053254378; fax: +1 4053255813.
E-mail address: mallinson@ou.edu (R.G. Mallinson).

cursor incorporated on to the support. The liquid/solid ratio used to achieve incipient wetness was 1.26 ml/g. The precursor was $\text{Pd}(\text{NO}_3)_2$, purchased from Sigma–Aldrich. After impregnation, the catalysts were dried overnight in an oven and then calcined in air at 400°C for 4 h. To study the effect of alkali addition, two catalysts were synthesized by adding controlled amounts of K onto the 10% Pd/SiO₂ catalyst.

2.2. Catalyst characterization

Dynamic pulse chemisorption was used to determine the Pd percent exposed. CO adsorption was conducted in a dynamic chemisorption unit, consisting of a pulse system with detection by an SRI Model 310C Gas Chromatograph equipped with a Thermal Conductivity Detector (TCD). All of the catalysts were reduced in H₂ by heating from ambient to 150°C with a ramp rate of $10^\circ\text{C}/\text{min}$, held for 1 h, then flushed with He for 30 min and cooled down to room temperature. A pre-mixed gas of 5% CO in He was used for pulse injection with a 0.1 ml loop size. Pulses of CO were sent over the catalyst at 25°C until breakthrough occurred and the size of the pulse peak no longer increased. The SiO₂ support was tested and no CO adsorption was detected.

Temperature Programmed Reduction (TPR) of 3% Pd/SiO₂ shows one peak centered at 50°C . Therefore, the changes observed after different reduction temperatures do not reflect different degrees of reduction, but rather morphological changes.

DRIFTS experiments were carried out in a PerkinElmer Spectrum 100 FTIR Spectrometer equipped with an MCT detector and a High Temperature Reaction Chamber (HVC-DRP) fitted with KBr windows (Harrick Scientific Products, Inc). The catalyst in an amount of 0.05–0.1 g was loaded to the reaction cell and reduced in H₂ flowing at 30 sccm by heating at a $10^\circ\text{C}/\text{min}$ ramp rate to 150°C or 250°C or 350°C , then holding for 1 h followed by flushing with He for 30 min before cooling to room temperature. CO (5% in He) then flowed through the chamber for 30 min at room temperature and was then flushed with He for 20 min before sample spectra were taken. Spectra were acquired at a resolution of 4 cm^{-1} averaging 64 scans.

2.3. Catalyst tests

Catalytic activity measurements were carried out in a continuous flow 0.75 cm I.D. stainless steel tubular reactor within an electric furnace. Runs were conducted for 2–3 h at 125°C and atmospheric pressure, using 0.05–0.15 g of catalyst and the appropriate flow rate to achieve the desired W/F (g cat/g feed/h). Hydrogen was used to reduce the catalyst and as a carrier gas for the organic feed that was delivered by a syringe pump into the gas stream, keeping a relative hydrogen to aldehyde and/or alcohol molar ratio of 12:1. The reactants used were: 2-methylpentanal (MPAL), 2-methylpentanol (MPOL), n-butanol (BOL), and n-propanal. Experiments co-feeding MPAL + MPOL, MPAL + BOL, n-propanal + MPOL, and n-propanal + MPAL were also conducted. The objective of carrying out different combinations will be discussed later. Heating tapes were used on all the lines to keep the feed and products in the vapor phase. Quantitative product analysis was made online in an HP 6890A gas chromatograph equipped with a flame ionization detector. Compositions of organic compounds are reported as mole fractions. A Shimadzu GCMS-QP2010S was used for product identification. The light gas products (mostly CO) were detected online via gas chromatography using a Carle series 400 AGC with TCD.

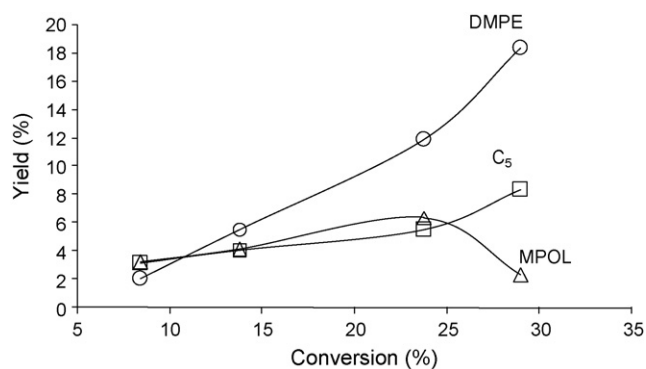


Fig. 1. Yields of products from MPAL on 16% Pd/SiO₂ reduced at 150°C and run at 125°C , 1 atm, H₂:MPAL = 12:1.

3. Results

3.1. Effect of varying feed composition

3.1.1. Pure aldehyde feed

2-Methylpentanal was fed on the 16% Pd catalyst reduced at 150°C to study the conversion of the aldehyde. The W/F was varied from 0.25 to 2 h to obtain conversions from 8.4% to 28.9%. The yields of products are plotted against conversion in Fig. 1. At low conversion, the major products are n-pentane (C₅) and MPOL that result from decarbonylation and hydrogenation, respectively. As the conversion increases, the yield of the ether (DMPE) becomes predominant, much higher than the yields of n-pentane and MPOL. The yield of MPOL decreases, suggesting that it is consumed to form the secondary product, DMPE. No other products were observed.

3.1.2. Pure alcohol feed

In order to compare the behavior of the aldehyde and alcohol, 2-methylpentanol was fed over the 16% Pd catalyst reduced at 150°C . The reactivity of MPOL was found to be considerably lower than that of MPAL and its conversion increases from 3.6% to 11.9% over longer W/F, from 1 to 4 h. The product yields are shown in Fig. 2. The products were DMPE, MPAL, n-pentane, and a small amount of 2-methylpentane (2MP). The yield of ether shows a slight induction period that could suggest that as the aldehyde increases, this enhances the rate of etherification. Some MPAL is formed from dehydrogenation while 2MP comes from dehydration of the MPOL, however the equilibrium greatly favors the alcohol at these conditions [19]. n-Pentane is produced from decarbonylation of the MPAL.

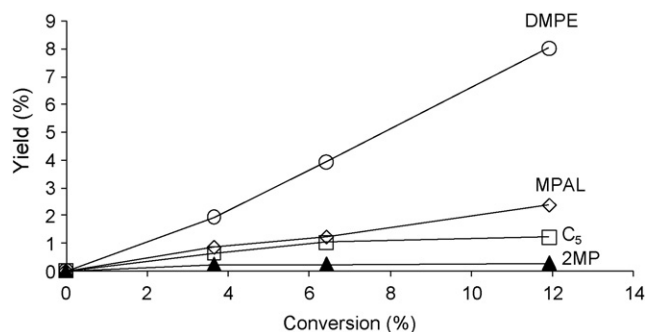


Fig. 2. Yields of products from MPOL on 16% Pd/SiO₂ reduced at 150°C and run at 125°C , 1 atm, H₂:MPOL = 12:1.

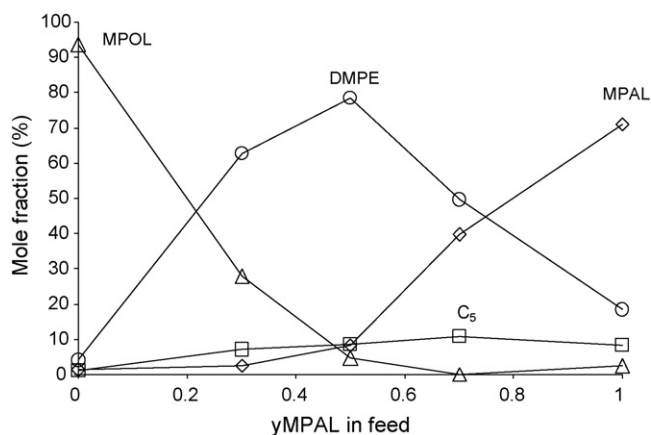


Fig. 3. Co-feed mixtures of MPAL and MPOL on 16% Pd/SiO₂ reduced at 150 °C and run at 125 °C, W/F = 2 h, H₂:feed = 12:1.

3.1.3. Mixtures of 2-methylpentanal with 2-methylpentanol at different feed ratios

When either the aldehyde or the alcohol is fed alone, the ether is the predominant product. Because under these reaction conditions a significant extent of inter-conversion of the two molecules may occur, both species may be present in every run. Therefore, it is unclear to what extent the etherification reaction depends upon the concentration of both species. To quantify the contribution of each one, experiments with mixed feeds at different ratios of MPAL and MPOL were carried out. The results for W/F = 2 h are shown in Fig. 3. A much higher ether yield was observed when using the mixtures than when using the pure feeds of either compound. The highest ether selectivity (90%) was achieved at a 1:1 feed molar ratio ($y_{\text{MPAL}} = 0.5$) with a yield, based upon conversion of both reactants, of 79%. These results show that etherification is enhanced when significant amounts of both MPAL and MPOL are present.

3.1.4. Mixtures of n-butanol and 2-methylpentanal

Because both MPAL and MPOL have the same alkyl chain, they produce a symmetric ether and the degree to which either aldehyde or alcohol may be incorporated is not made clear from the above results. Therefore, n-butanol and 2-methylpentanal were co-fed at a 1:1 volume ratio (1.3:1 molar ratio), respectively. The composition of feeds and products are shown in Fig. 4 with increasing W/F. The results show that both C₁₀ and C₁₂ (DMPE) ethers are the major products, but only a trace of C₈ ether. MPAL is also consumed to a minor extent by decarbonylation and hydrogenation. The comparative rates for C₁₀ and C₁₂ ether formation are best shown by the

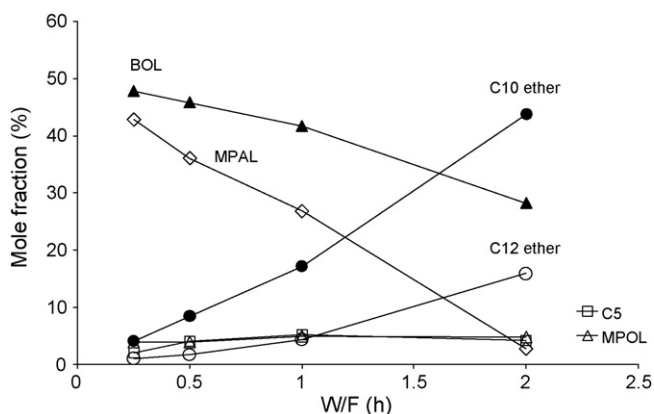


Fig. 4. Cross etherification of n-butanol and 2-methylpentanal on Pd reduced at 150 °C and run at 125 °C, $y_{\text{MPAL}} = 0.43$, H₂:feed = 12:1.

Table 1

Etherification product mole fraction of mixed feeds of aldehydes + alcohols on 16% Pd/SiO₂, reduced at 150 °C and run at 125 °C; molar H₂:feed ratio = 12:1; molar MPAL:MPOL ratio = 1:1; molar MPAL:n-butanol ratio = 1:1.3; molar propanal:MPOL ratio = 1:1; molar propanal:MPAL ratio = 1:1.

Feed	Ether product mole fraction				
	C ₆	C ₈	C ₉	C ₁₀	C ₁₂
MPAL + MPOL					78.5
MPAL + n-butanol		0.02		43.8	15.9
Propanal + MPOL	0.05		47.5		2.28
Propanal + MPAL	0.09		11.3		2.11

ratio of the two at very low W/F; in this case 0.25 and 0.5 h are used. This ratio is 5.0 for C₁₀/C₁₂. MPAL reacts readily with BOL to form the C₁₀ ether. The alcohol is highly reactive for ether formation with an aldehyde, but has low reactivity for other reactions, whereas the aldehyde decarbonylates and hydrogenates to some extent, giving it a higher rate of conversion.

3.1.5. Mixtures of n-propanal and 2-methylpentanal

A similar experiment to study cross etherification was carried out for a mixed feed of C₃AL (n-propanal) with MPOL, at a molar ratio of 1:1 on 16% Pd/SiO₂ reduced at 150 °C and run at 125 °C with a W/F = 2 h. The cross C₉ ether yield was 47.5%, much higher than the C₆ and C₁₂ ethers whose yields are 0.05% and 2.28%, respectively. This result also confirms the high yield of the mixed ether, similar to the previous experiment when feeding both BOL + MPAL. The results of ether formation from the mixed feed experiments are summarized in Table 1.

3.1.6. Mixtures of n-propanal and 2-methylpentanal

From previous mixed feed experiments, it is clear that high yields of the cross ether are achieved when reacting an aldehyde and an alcohol. This confirms the hypothesis that etherification requires both adsorbed aldehyde and alcohol with abundant amounts on the surface. However, it remains unclear if etherification can proceed to a significant extent without an alcohol in the system. Therefore, an experiment with a mixed feed of only aldehydes in the absence of hydrogenation will help demonstrate whether this occurs.

Experiments were conducted with n-propanal and 2-methylpentanal and with either He or H₂ as the carrier gas. In a He carrier, no hydrogenation or ether formation was observed and the only reaction observed was decarbonylation of the aldehydes to hydrocarbons. In a H₂ carrier, the observed products are hydrogenated alcohols from the corresponding aldehydes, as well as hydrocarbons and ethers. The yields of ethers are much smaller than feeding mixed alcohol and aldehyde. Yields of C₉ and C₁₂ ethers are 11.3% and 2.11%, respectively. The C₆ ether yield is much smaller than the others, and very little propanal is observed compared to MPOL. This could indicate either that the propanal is not effectively hydrogenated and the C₉ ether is produced from propanal and MPOL or that the propanal is readily hydrogenated and reacts with the MPAL to form the C₉ ether.

An experiment using only propanal as a feed was conducted under the same conditions as the other experiments. As shown in Table 2, when compared at the same conversion level (24%), much less etherification was observed with propanal than with methylpentanal, while the hydrogenation to propanol was substantially higher than for the larger aldehyde.

Table 2

Etherification of propanal or 2-methylpentanal at 125 °C on 16% Pd/SiO₂ reduced at 150 °C, molar H₂:feed = 12:1.

Feed	Propanal	2-Methylpentanal (MPAL) ^a	
W/F (h)	2	1	
Conversion (%)	23.8	23.8	
Yield (%)			
Ethane	2.5	n-Pentane	5.5
Propanol	14.6	MPOL	6.4
Dipropylether	6.7	DMPE	11.9
Ether/hydrocarbon ratio	2.7	2.2	

^a Data from Fig. 1.

3.2. Effect of metal loading on 3, 10 and 16 wt.% Pd/SiO₂

Catalysts with different metal loadings, reduced at 150 °C, were compared for etherification at similar levels of conversions of 2-methylpentanal. As shown in Table 3, CO chemisorption measurements indicate that increasing the loading from 3 to 16 wt.% resulted in increased particle size. The estimated aldehyde reaction rate per surface atom is similar for the three catalysts. The ether yield and selectivity are highest for the 16 wt.% Pd catalyst, also shown in Table 3. The other major products are n-pentane, which is produced by decarbonylation, and 2-methylpentanol from hydrogenation.

3.3. Effect of reduction temperature

When the 3 wt.% Pd was reduced at 150 °C, the yield of ether was 7.2% at W/F = 2 h, lower compared to the ether yields for the 10% Pd (7.7%) and 16% Pd (11.9%), as shown in Table 3. However, when the reduction temperature of the 3% Pd was increased from 150 °C to 200 °C and 250 °C for experiments at a conversion of about 20%, the ether yield was found to increase from 7.2% to 9.2% and 10.2%, respectively, as shown in Table 4. When the reduction temperature was increased to 200 °C for the 16% Pd, an increased ether yield from 11.9% to 13.1% was observed, even while the conversion was reduced from 23.8% to 20%.

3.4. Effect of alkali addition

The results obtained on the K-containing catalysts are summarized in Table 5. It is observed that even at half the space velocity, the conversion on the K-doped catalysts is significantly lower than that obtained on the K-free Pd catalyst. The etherification selectivity decreases with the addition of K, while that of decarbonylation greatly increases.

Table 3

Activity of 3, 10 and 16 wt.% Pd/SiO₂ reduced at 150 °C with product yields from MPAL conversion at 125 °C, molar H₂:MPAL ratio = 12:1.

Catalyst	3% Pd	10% Pd	16% Pd
Dispersion (%)	7.10	5.30	3.90
W/F (h)	2	1	1
Conversion (%)	20.9	20.4	23.8
TOF (molecule/sites)	1.44E-02	1.13E-02	1.14E-02
Yield (%)			
n-Pentane	7.0	5.3	5.5
MPOL	6.7	7.4	6.4
C ₁₂ ether	7.2	7.7	11.9
Selectivity (%)			
n-Pentane	33.4	26.0	23.1
MPOL	32.0	36.4	26.8
C ₁₂ ether	32.6	37.6	50.1

Table 4

Effect of reduction temperature of 3% Pd and 16% Pd catalysts on MPAL conversion at 125 °C, molar H₂:MPAL ratio = 12:1.

Catalyst	3% Pd			16% Pd	
	150 ^a	200 ^a	250 ^a	150 ^a	200 ^a
W/F (h)	2	2	2	1	1
Conversion (%)	20.9	24.2	22.7	23.8	20.0
Yield (%)					
n-Pentane	7.0	5.1	5.3	5.5	6.4
MPOL	6.7	10.1	7.2	6.4	0.6
C ₁₂ ether	7.2	9.1	10.2	11.9	13.1
Selectivity (%)					
n-Pentane	33.4	21.0	23.2	23.1	31.7
MPOL	32.0	41.6	31.7	26.8	3.0
C ₁₂ ether	34.6	37.4	45.1	50.1	65.3

^a T_{reduction} (°C).

Table 5

Effect of K addition to 10% Pd/SiO₂ catalysts in the 2-methylpentanal conversion at 125 °C, molar H₂:MPAL ratio = 12:1, after reduction at 150 °C.

Catalyst	10% Pd	0.2% K-10% Pd	2% K-10% Pd
W/F (h)	1	2	2
Conversion (%)	20.4	14.9	9.8
Selectivity (%)			
n-Pentane	26.0	55.7	95.0
MPOL	36.4	25.5	4.2
C ₁₂ ether	37.6	18.8	0.8

3.5. In situ DRIFTS

The spectra from CO chemisorption on 3% Pd at different reduction temperatures are shown in Fig. 5. The peaks at 1980 and 1940 cm⁻¹ are assigned to bridge and multibonded CO species, respectively, typical of relatively large particles, in agreement with the metal dispersions estimated from chemisorption measurements [20,21]. The much weaker band ascribed to linear CO appearing at around 2070 cm⁻¹ [22,23] overlaps with the two branches resulting from residual gas phase CO remaining in the optical path after flushing with He for 20 min. As the reduction temperature increases, not only do both the bridge and multibonded CO peaks become relatively larger, but the multibonded-to-bridge ratio also increases. The bridge form is mostly associated with the presence of Pd(100) faces in the metal particle [24,25] while the multibonded species is more typical of Pd(111) faces [24,25]. This tendency is not only consistent with an increase in metal particle

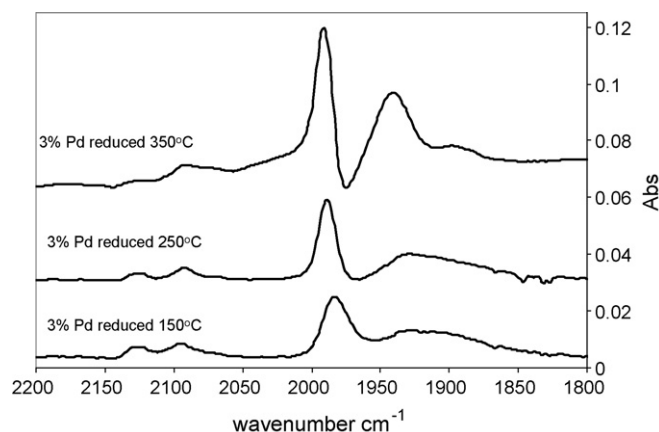


Fig. 5. FTIR of CO on 3% Pd reduced at 150 °C, 250 °C and 350 °C.

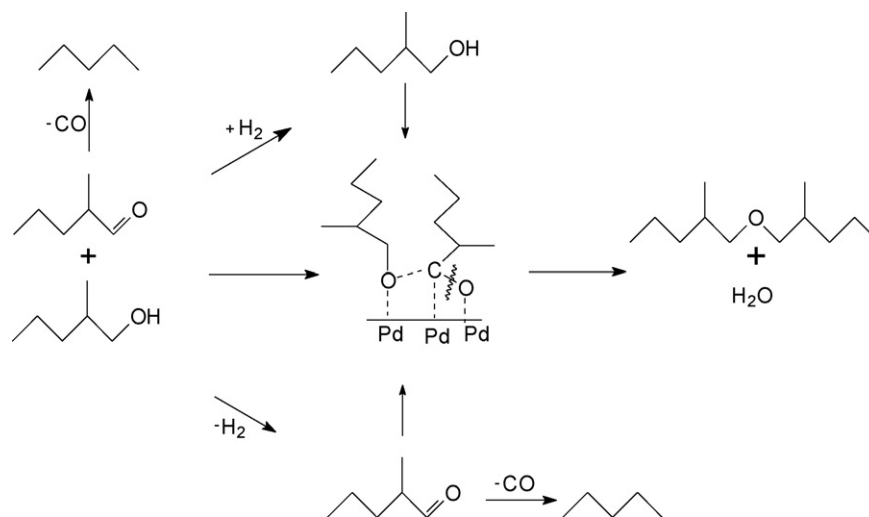


Fig. 6. Schematic reaction pathway of 2-methylpentanal on Pd catalyst.

size, but also with a smoothing of the surface caused by the crystal annealing occurring as the reduction temperature increases.

4. Discussion

In early work that is very relevant to the current study, Ponec and co-worker [16] observed the production of ether when pulsing different mixtures of alcohol and aldehyde over metal catalysts. In agreement with that work, we show here that when fed individually, both aldehydes and alcohols form ethers. However, etherification is significantly enhanced when both are fed simultaneously. When only one is present in the feed, etherification apparently occurs due to the inter-conversion of aldehyde to alcohol or vice versa. The proposed reaction pathways are shown in Fig. 6.

As mentioned above, because both the aldehyde and alcohol have the same methylpentyl alkyl group, the resulting ether is symmetric and the relative contribution of each is not discernable. The results from the mixture experiment with MPAL and BOH clearly show that both are required to maximize ether, confirming the results of the MPAL–MPOL experiments. This condition suggests that each oxygenate forms a unique surface intermediate that is needed for the formation of the ether bond and is not efficiently inter-converted. An alcohol molecule is typically adsorbed on metal surfaces as an alkoxide. When an aldehyde is adsorbed as an $\eta^2(\text{C},\text{O})$ species adjacent to the alkoxide [17,18,26], this enables the formation of a C–O–C bond generating an ether [14,16]. Accordingly, etherification should be favored on metal catalysts that promote the co-existence of both species. Under these conditions, the η^2 adsorbed C–O may cleave and the ether bond is formed with the alkoxide oxygen [14,26]. The residual oxygen from the aldehyde is removed from the surface as water in the presence of hydrogen. The formation of this surface hydroxyl should provide the driving force for the oxygen cleavage from the adsorbed aldehyde carbon, allowing formation of the ether bond.

Formation of the alkoxide species is a relatively easy process that most metal surfaces are able to promote [27–29]. On Pt-group metals (including Pt [30,31], Ni [32] and Pd [33]), adsorption of alcohols results in the formation of an alkoxide on the surface via hydroxyl-hydrogen elimination, followed by α -hydrogen abstraction that leads to an aldehyde intermediate bonded onto the surface via both carbon and oxygen atoms (in an $\eta^2(\text{C},\text{O})$ configuration) or an oxygen atom only ($\eta^1(\text{O})$ configuration), as illustrated in Fig. 7. Kinetic experiments for CH_3OH decomposition on Ni(111) and Ni(110)

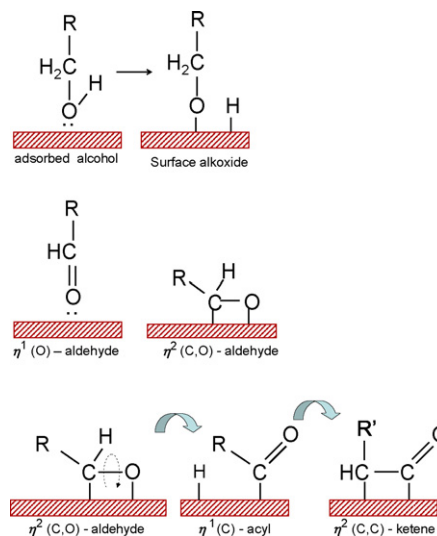


Fig. 7. Adsorption modes of alcohols and aldehydes on Pd(111) and sequence from $\eta^2(\text{C},\text{O})$ -aldehyde to $\eta^2(\text{C},\text{C})$ -ketene of decarbonylation [26].

surfaces [34,35] revealed that the cleavage of the C–H bond of the methoxide is the rate-limiting step in methanol decomposition to surface H_2CO species. They also found the same results when using ethanol.

In contrast to alkoxides, the surface species that result from the adsorption of aldehydes strongly depends on the type of metal used. On Group IB metals, aldehydes adsorb exclusively in an η^1 configuration, but they adsorb in both η^1 and η^2 configurations on Group VIII metals at a ratio that strongly depends on the specific metal [27]. In the former configuration, the aldehyde binds to the surface through the O lone pair, while in the latter it binds through the π orbital of the carbonyl, overlapping the d electrons from the metal with the antibonding π^* orbital in the carbonyl. As a result, when there is significant back-donation from the metal, this configuration can be readily stabilized [26]. Therefore, the preference to form either η^1 or η^2 surface species can be explained by these electronic characteristics of the metal. For example, the much greater η^2/η^1 ratio observed on Ru compared to Pt has been ascribed to a higher extent of this electron back-donation from the metal to the π^* orbital of carbonyl, resulting from the higher position of the Fermi level in Ru compared to Pt. It is well known that a more efficient transfer of an electron into the antibonding states of the

molecule's π system enhances the strength of interaction with the metal, while it weakens the C–O bond, favoring the η^2 mode.

In the specific case of Ru, it has been observed [29] that while η^2 is the preferred adsorption species on clean Ru surfaces, only η^1 is present on oxygen-covered surfaces. Those authors proposed that while the hindrance of η^2 formation can be ascribed to simple geometric blockage of sites, electronic effects are much more significant in determining which configuration is preferred [27]. It is expected that co-adsorption of an electronegative atom results in an increase in the work function of the metal, lowering the Fermi level and making back-donation less favorable. By contrast, they have observed that η^2 species are favored by co-adsorption of K, which causes a decrease in work function. It is also expected that the specific surface plane on which the aldehyde adsorbs will affect the type of surface species formed.

In this contribution, we have demonstrated that the generation of smooth planes (e.g. Pd(1 1 1)) on the particle surface by increasing either the metal loading or the reduction temperature results in a higher etherification rate. This enhancement in rate cannot be due to a higher concentration of η^2 species, since it cannot be expected that Pd(1 1 1) planes result in a higher η^2/η^1 ratio. In fact, it has been recently shown [36–38] that in high-coordination smooth surfaces, the d-band center is located at a lower energy, farther from the Fermi level than rougher surfaces with lower coordination numbers. Accordingly, one may expect that a catalyst with larger and smoother Pd particles, such as those present in the high Pd loading samples studied here, particularly after high temperature reduction, should not present a higher concentration of η^2 species than a catalyst with smaller and rougher particles. Therefore, the enhanced etherification activity of these surfaces must be ascribed to their ability to co-adsorb the two required species on adjacent sites rather than an enhanced ability to adsorb either one.

The 16 wt.% Pd, with the largest particle size, may have a higher density of large ensembles necessary for condensation to form the ether (DMPE), thus increasing its yield, while decreasing the yields of the other products. The increased ether yield with increasing reduction temperature, suggests that the Pd surface anneals into thermodynamically more stable surfaces (i.e. (1 1 1)), resulting in a surface structure having larger ensembles that are selective for ether formation. The FTIR results show structural changes to the surface that are consistent with this view.

The decarbonylation reaction requires further transformation of an $\eta^2(\text{C,O})$ species with its conversion to an $\eta^1(\text{C})$ acyl configuration with the O angled away from the surface (by further H-abstraction by the metal) [26]. This then may form an $\eta^2(\text{C,C})$ ketene with the adjacent C bonding to the surface [26]. C–C bond scission occurs, leaving the alkyl fragment and CO [26]. The ether yield is higher than the decarbonylated C_5 hydrocarbon because the ether is more readily formed when there are adjacent surface alkoxides.

The experiments conducted on K-promoted catalysts further support the explanations given above and add another important concept to the discussion. In the first place, as mentioned above, the presence of K on Pd surfaces should result in an increased concentration of η^2 species [27]. However, this increase does not result in enhanced etherification activity, but rather a decrease that may be explained by the dilution of the ensemble site necessary for the bimolecular surface reaction. A final interesting point is the dramatic increase in selectivity for decarbonylation observed for the 2% K-doped catalyst. This selectivity change may be associated not only with an electronic modification of the Pd activity, but also to a direct participation of K in the reaction interacting directly with the carbonyl oxygen of the aldehyde and enhancing its C–C bond cleavage.

5. Conclusion

The etherification reaction has been studied for various aldehydes and alcohols on supported Pd catalysts. While alcohols adsorb as alkoxide species on the surface, aldehydes adsorb as $\eta^2(\text{C,O})$. For high rates of ether formation, it is necessary to have both alkoxide and η^2 -adsorbed species on the surface and a stoichiometric mixture of 1:1 of aldehyde and alcohol has been found to be the optimum.

Larger metal particles, that have been sintered and annealed by high reduction temperatures, show lower conversion but higher ether selectivity due to enhancement of the ensembles required for etherification.

Acknowledgments

The support of the Oklahoma Secretary of Energy, the Oklahoma Bioenergy Center, The National Science Foundation EPSCoR (0814361), and the Department of Energy (DE-FG36G088064) are gratefully acknowledged.

References

- [1] J.N. Chheda, J.A. Dumesic, *Catal. Today* 123 (2007) 59–70.
- [2] R.M. West, Z.Y. Liu, M. Peter, C.A. Gärtner, J.A. Dumesic, *J. Mol. Catal. A* 296 (2008) 18–27.
- [3] T. Sooknoi, T. Danuthai, L.L. Lobban, R.G. Mallinson, D.E. Resasco, *J. Catal.* 258 (2008) 199–209.
- [4] M. Snare, I. Kubickova, P. Maki-Arvela, D. Chichova, K. Eranen, D.Y. Murzin, *Fuel* 87 (2008) 933–945.
- [5] L. Karas, W.J. Piel, "Ethers", *Kirk-Othmer Encyclopedia of Chemical Technology*, John Wiley & Sons, Inc., 2004, pp. 567–583.
- [6] G.A. Olah, US Patent 5,520,710 (1996).
- [7] E.W. Flick, *Industrial Solvents Handbook*, 5th edition, 1998.
- [8] R.J.J. Nel, A. De Klerk, *Ind. Eng. Chem. Res.* 48 (2009) 5230–5238.
- [9] A. Corma, M. Renz, *Angew. Chem. Int. Ed.* 46 (2007) 298–300.
- [10] R.H. Clark, W.E. Graham, A.G. Winter, *J. Am. Chem. Soc.* 47 (1925) 2748–2754.
- [11] R. Figueras Roca, L. De Mourgues, Y. Trambouze, *J. Catal.* 14 (1969) 107–113.
- [12] H. Feuer, J. Hooz, in: S. Patai (Ed.), *The Chemistry of the Ether Linkage*, Interscience, London, 1967, pp. 457–460.
- [13] T.P. Kobylinski, H. Pines, *J. Catal.* 17 (1970) 384–393.
- [14] A. van der Burg, J. Doornbos, N.J. Kos, W.J. Ultee, V. Ponec, *J. Catal.* 54 (1978) 243–253.
- [15] G.M.R. van Druten, V. Ponec, *Appl. Catal. A* 191 (2000) 153–162.
- [16] G.M.R. van Druten, V. Ponec, *Appl. Catal. A* 191 (2000) 163–176.
- [17] F. Delbecq, P. Sautet, *Surf. Sci.* 295 (1993) 353–373.
- [18] R. Shekhar, M.A. Barteau, R.V. Plank, J.M. Vohs, *J. Phys. Chem. B* 101 (1997) 7051–7939.
- [19] T.T. Pham, L.L. Lobban, D.E. Resasco, R.G. Mallinson, *J. Catal.* 266 (2009) 9–14.
- [20] A. Palazov, C.C. Chang, R.J. Kokes, *J. Catal.* 36 (1975) 338–350.
- [21] A. Arteaga, F.M. Hoffmann, A.M. Bradshaw, *Surf. Sci.* 119 (1982) 79–94.
- [22] L.L. Sheu, Z. Karpinski, W.M.H. Sachtler, *J. Phys. Chem.* 93 (1989) 4890–4894.
- [23] F. Skoda, M.P. Astier, G.M. Pajonk, M. Primet, *Catal. Lett.* 29 (1994) 159–168.
- [24] M. Fernandez-Garcia, J.A. Anderson, G.L. Haller, *J. Phys. Chem.* 100 (1996) 16247–16254.
- [25] F.M. Hoffmann, *Surf. Sci. Rep.* 3 (1983) 107–192.
- [26] M. Mavrikakis, M.A. Barteau, *J. Mol. Catal. A* 131 (1998) 135–147.
- [27] N.R. Avery, W.H. Weinberg, A.B. Anton, B.H. Toby, *Phys. Rev. Lett.* 51 (1983) 682–685.
- [28] N.R. Avery, *Surf. Sci.* 125 (1983) 771–786.
- [29] A.B. Anton, N.R. Avery, B.H. Toby, W.H. Weinberg, *J. Am. Chem. Soc.* 108 (1986) 684–694.
- [30] J.L. Davis, M.A. Barteau, *Surf. Sci.* 187 (1987) 387–406.
- [31] J.L. Davis, M.A. Barteau, *Surf. Sci.* 235 (1990) 235–248.
- [32] S.M. Gates, J.N. Russell Jr., J.T. Yates Jr., *Surf. Sci.* 171 (1986) 111–134.
- [33] B.A. Sexton, K.D. Rendulic, A.E. Hughes, *Surf. Sci.* 121 (1982) 181–198.
- [34] S.R. Bare, J.A. Strosio, W. Ho, *Surf. Sci.* 150 (1985) 399–418.
- [35] S.M. Gates, J.N. Russell Jr., J.T. Yates Jr., *Surf. Sci.* 159 (1985) 233–255.
- [36] B. Hammer, J.K. Nørskov, *Adv. Catal.* 45 (2000) 71–129.
- [37] M. Mavrikakis, B. Hammer, J.K. Nørskov, *Phys. Lett.* 81 (1998) 2819–2822.
- [38] C.E. Tripa, T.S. Zubkov, J.T. Yates Jr., M. Mavrikakis, J.K. Nørskov, *J. Chem. Phys.* 111 (1999) 8651–8658.